Bi-level Coordinated Planning of Active Distribution Network Considering Demand Response Resources and Severely Restricted Scenarios

Yixin Huang, Zhenzhi Lin, Xinyi Liu, Li Yang, Yangqing Dan, Yanwei Zhu, Yi Ding, and Qin Wang

***Abstract*—Due to the uncertainty and fluctuation of distributed generation (DG) and load, the operation of active distribution network (ADN) is affected by multi-dimension factors which are described by massive operation scenarios. Efficient and accurate screening of severely restricted scenarios (SRSs) has become a new challenge in ADN planning. In this paper, a novel bi-level coordinated planning model which combines the short-time-scale operation problem with the long-time-scale planning problem is proposed. At the upper level, the demand response (DR) resource, an effective non-component planning resource characterized by low capacity price, high energy price, and short contract term, is co-optimized with the configuration of lines and energy storage systems (ESSs) to achieve the economic trade-off between the investment cost and the operation cost under SRSs. At the lower level, with the planning scheme obtained from the upper level, massive operation problems are optimized to minimize the daily operation cost; and the SRSs are provided to the upper level through a shadow-price-based scenario screening method, which simulates the planning information (i.e., the restricted degrees of operation scenarios) feedback process from ADN operators to ADN planners. Case studies on a 62-node distribution system in Jianshan New District, Zhejiang Province, China, illustrate the effectiveness of the proposed bi-level coordinated planning model considering DR resources and SRSs.**

***Index Terms*—Active distribution network, demand response resource, bi-level coordinated planning, severely restricted scenario screening, shadow price.**

Manuscript received: May 25, 2020; accepted: September 3, 2020. Date of CrossCheck: September 3, 2020. Date of online publication: March 9, 2021.

This work was supported by the National Key R&D Program of China (No. 2016YFB0900100), the National Natural Science Foundation of China (No. 51777185), and the Science and Technology Program of State Grid Zhejiang Electric Power Co., Ltd. (No. 5211JY180015).

Y. Huang, Z. Lin (corresponding author), X. Liu, L. Yang, and Y. Ding are with the College of Electrical Engineering, Zhejiang University, Hangzhou, China (e-mail: ee_hyx@zju.edu.cn; linzhenzhi@zju.edu.cn; ee_lxy@126.com; eeyangli@zju.edu.cn; yiding@zju.edu.cn).

Y. Dan is with State Grid Zhejiang Economic Research Institute, Hangzhou, China (e-mail: danyangqing@aliyun.com).

Y. Zhu is with State Grid Ningbo Power Supply Company, Hangzhou, China (e-mail: zhuyw99@163.com).

Q. Wang is with the Electric Power Research Institute, Palo Alto, USA (e-mail: qwang@epri.com).

DOI: 10.35833/MPCE.2020.000335

NOMENCLATURE

A. Indices and Sets

τ	Index for iteration
Ω_{Eline}, Ω_{Lline}	Sets of existing and loop lines
Ω_{EESS}, Ω_{NESS}	Sets of nodes with existing energy storage system (ESS) and ESS newly installed
Ω_{line}	Set of line
Ω_m	Set of load type
Ω_{Nline}, Ω_{Rline}	Sets of newly-installed and reinforced candidate lines
Ω_{Nlr}, Ω_{Rlr}	Sets of types of newly-installed and reinforced candidate lines
Ω_{node}, Ω_{node}^m	Sets of node and node of load type m
Ω_s, Ω_{s*}	Sets of operation scenarios and severely restricted scenarios (SRSs)
Ω_{sub}	Set of substation node
Ω_u, Ω_l	Sets of decision variables of upper-level and lower-level models
a, b, c	Indices for demand response (DR) provider type
i, j, k	Indices for nodes
m	Index for load type
n	Index for planning stage
r	Index for line type
s, $s*$	Indices for operation and severely-restricted scenarios
t	Index for time period

B. Parameters

$\alpha_{n,m,i}^{DR}$	The maximum potential coefficient of DR resource provider at node i of load type m at planning stage n
$\alpha_{n,m,\max}^{DR}$	The maximum potential coefficient of load type m at planning stage n
γ_{ch}, γ_{dis}	Charging and discharging efficiencies of ESS
Δt	Duration of time period
δ	Conversion coefficient

ε	Self-discharging rate
ζ_s	Scenario impact factor of scenario s
ζ_0	Threshold of scenario impact factor
θ_{PV}, θ_{WT}	The maximum curtailment rates of photovoltaic (PV) and wind turbine (WT)
λ	The maximum load shedding rate
$\mu_{s,m,i,t}$	Lagrange multiplier of the upper limit of DR power constraint at time period t at node i with load type m in scenario s
$\pi_{s,j,t}$, $\tau_{s,j,t}$	Lagrange multipliers of power and stored energy constraints of ESS at node i at time period t in scenario s
ρ	Discount rate
σ_{ij}	Reactance of line ij
Ψ_s	Shadow price of scenario s
$v^u_{s,ij,t}$, $v^d_{s,ij,t}$	Lagrange multipliers of line ij power flow constraints at time period t in scenario s
C_{total}	Total planning cost
C_{s*}	Total dispatching cost under SRSs
C^{cap}	DR capacity cost
C^{ene}_s	DR energy cost in scenario s
C^{inv}_{line}, C^{inv}_{ESS}	Investment costs of line and ESS
$C^{inv}_{\max}$, C^{inv}_n	The upper limit and actual value of investment cost at planning stage n
C^{loss}_s	Power loss cost in scenario s
C^m_{line}, C^m_{ESS}	Maintenance costs of line and ESS
C^{ope}_s	Daily operation cost in scenario s
C^{ope}_{target}	Operation cost in the target year
$C^{penalty}_s$	Penalty cost for PV and WT curtailment and load shedding in scenario s
C^{pur}_s	Energy purchase cost in scenario s
c_r	Unit investment cost of line type r
$c^{cap}_{n,m,i}$	Unit DR capacity price at node i of load type m at planning stage n
$c^{cap}_{n,m,dead}$, $c^{cap}_{n,m,sat}$	Boundary points of the dead and saturated zones of load type m at planning stage n
$c^{ene}_{m,i}$	Unit DR energy price at node i of load type m
c^m_{line}, c^m_{ESS}	Unit maintenance costs of line and ESS
$c^{NESS}_{S,i}$, $c^{ESS}_{P,i}$, $c^{ESS}_{E,i}$	Fixed construction cost, unit rated power cost, and unit capacity cost of ESS at node i
c^{PVP}, c^{WTP}, c^{shed}	Unit penalty costs of PV curtailment, WT curtailment, and energy not supplied
c^{pur}_t	Unit electricity price at time period t
$E^{ESS}_{i,\max}$	The maximum rated capacity of expanded ESS at node i at planning stage n
$E^{SOC}_{i,\min}$, $E^{SOC}_{i,\max}$	The minimum and maximum stored energy limits of ESS at node i
$K^{DR}_{n,m}$	Sensitivity coefficient of DR resource provider of load type m at planning stage n
L_{ij}	Length of line ij
M	Sufficiently large positive number
N_{LS}	Number of lines in the line set with a loop structure
N_s	Number of operation scenarios
N_T	Number of planning stages
$P^{DR}_{n,m,\min}$	The minimum hourly DR power of DR resource provider of load type m at planning stage n
$P^{ESS}_{i,\max}$	The maximum rated power of expanded ESS at node i at planning stage n
$\overline{P}^{load}_{n,m,i}$	The maximum load power at node i of load type m at planning stage n
$\overline{P}^{PV}_{s,i,t}$, $\overline{P}^{WT}_{s,i,t}$	The maximum output power of PV and WT at node i at time period t in scenario s
p_s	Probability of scenario s
r_{ij}	Resistance of line ij
$S^{line}_{n,ij}$	The maximum capacity of line ij at planning stage n
T	Number of time periods in a dispatch cycle
$T^{DR}_{\max}$	The maximum duration of DR event period
$t^{start}_{m,i}$, $t^{end}_{m,i}$	Start time and end time of DR event period at node i of load type m
$V_{i,\min}$, $V_{i,\max}$	The lower and upper voltage limits at node i
Y^{line}, Y^{ESS}	Lifecycles of line and ESS

C. Variables

$E^{ESS}_{n,i}$	Rated capacity of expanded ESS at node i at planning stage n
$E^{SOC}_{s,i,t}$	State of charge of ESS at node i at time period t in scenario s
$I_{s,ij,t}$	Current flowing through line ij at time period t in scenario s
$I^{\varphi}_{s,ij,t}$	Square of current flowing through line ij at time period t in scenario s
$P_{s,j,t}$, $P^{char}_{s,j,t}$, $P^{dis}_{s,j,t}$	Active nodal injection power, ESS charging power, and ESS discharging power at node j at time period t in scenario s
$P^{cap}_{n,m,i}$	Contract capacity signed with the DR resources provider at node i of load type m at planning stage n
$P^{DR}_{s,m,i,t}$	Active DR power at time period t at node i of load type m in scenario s
$P^{ESS}_{n,i}$	Rated power of expanded ESS at node i at planning stage n
$P^{line}_{s,ij,t}$	Active power through line ij at time period t in scenario s
$P^{loss}_{s,ij,t}$	Power loss of line ij at time period t in scenario s
$P^{pur}_{s,i,t}$	Active power purchased from the upper grid at node i at time period t in scenario s
$P^{PV}_{s,i,t}$, $P^{WT}_{s,i,t}$, $P^{shed}_{s,i,t}$	Active power of PV, WT, and load shedding at node i at time period t in scenario s

$Q_{s,j,t}$, $Q_{s,j,t}^{pur}$, $Q_{s,j,t}^{CB}$ Reactive nodal injection power, power purchased from the upper grid and compensation power at node j at time period t in scenario s

$Q_{s,ij,t}^{line}$ Reactive power through line ij at time period t in scenario s

$Q_{s,j,t}^{load}$, $Q_{s,j,t}^{PV}$, $Q_{s,j,t}^{WT}$ Reactive power of load, WT, and PV at node j at time period t in scenario s

$V_{s,i,t}$ Nodal voltage at node i at time period t in scenario s

$V_{s,ij,t}^{\varphi}$ Square of nodal voltage at node i at time period t in scenario s

$x_{s,i,t}^{dis}$, $x_{s,i,t}^{char}$ Binary variables for representing the utilization state of ESS at node i at time period t in scenario s

$x_{s,i}^{NESS}$ Binary variable for representing the investment state of ESS newly installed at node i at planning stage n

$x_{n,ij}^{line}$ Binary variable for representing the investment state of line ij at planning stage n

$y_{n,ij}^{line}$ Binary variable for representing the utilization state of line ij at planning stage n

I. Introduction

NOWADAYS, more distributed generations (DGs) such as photovoltaic (PV) and wind turbine (WT) are connected to the distribution network due to their advantages of low carbon emissions, high efficiency, and high flexibility [1], which brings in numerous operation scenarios with high risks but low probabilities [2], [3]. In some of these operation scenarios, the inadequate ability of the distribution network to consume renewable energy raises requirements for expensive additional investments [4]. The optimal dispatching of energy storage system (ESS) [5], [6], electric vehicle (EV) [7], combined heat and power (CHP) unit [8], and demand response (DR) [9] is considered in active distribution network (ADN) operation and planning, which not only reduces the operation risks caused by the mass connection of DGs, but also improves the economic performance of the distribution network planning scheme.

The economy, reliability, and flexibility of ADN can be improved by optimal planning and dispatching of DG [10], [11]. Considering the active management of DG, a multi-stage ADN planning model is proposed in [12] to decide the installation location, capacity and time of substations, lines, capacitors, and voltage regulators. In [13], the DG investment is integrated with a multi-stage planning model of lines and substations to reduce the investment cost. To handle the uncertainties caused by DG and load [14], [15], the stochastic theory [16]-[19] and robust theory [20]-[22] are widely applied in ADN planning models. In [21] and [22], robust distribution network planning models are proposed considering the uncertainty of the demands of load and EV. Based on the stochastic theory, the uncertain characteristics of loads and DGs are modeled with probability distribution functions. In [23], the uncertain forecasting errors of DGs are described with Gaussian distribution to obtain the confidence intervals of the forecasting load. With the development of the multi-scenario technique, the uncertainties of ADN planning are described as probabilistic scenarios. Based on the multi-load scenarios obtained from the forecasting data, an ADN planning model is presented in [16] to obtain the optimal reconfiguration of lines and DGs for power system planners, as well as the economic dispatching of DG and the topology reconfiguration for grid companies. In [17], based on several representative scenarios describing the uncertainty of DG and load, a bi-level ADN planning model is proposed to determine the distribution network frame at the upper level and the DG optimal configuration at the lower level. The correlated uncertainty of DG and load is represented with equiprobable scenarios in the stochastic programming model proposed in [18]. To avoid the computational burden [24], only several predetermined scenarios rather than massive scenarios are considered in [16]-[18]. It is difficult for ADN operator to identify all scenarios which should be considered in ADN planning based on experience. In power system economics, the shadow prices of active constraints reflect the marginal values of an optimal operation cost [25], [26]. The scarcity of an ADN planning resource in an operation scenario is quantitatively assessed by the shadow price, which further reflects the restricted degree of the scenario, i.e., the value and necessary level to be considered in the ADN planning. In this paper, a shadow price-based scenario screening method is proposed to screen out the necessary scenarios for ADN planning.

The impacts of price-based DR programs such as time of use (TOU) program [27] and real-time pricing (RTP) program [28], [29] are investigated in existing ADN planning models. The load adjustment can be achieved based during different TOU pricing strategies at different time periods [30]. In [31], different TOU pricing strategies at different time periods are incorporated in the ADN planning model to postpone the investment. In [32], the influences of different TOU-based DR policies and penetration rates on possible benefits and overcharges are considered in the proposed ADN planning model with the minimum investment and operation costs. In [33], the RTP-based DR is integrated with the planning model to balance load and electricity supply in the ADN with high penetration of DG. In [34], [35], the planning models considering the own-price and cross-price elasticities of RTP-based DR are established to determine the investment of ADN components. It can be seen that the DR is considered in the short-term operation problems in the ADN planning scheme only, rather than as a long-term non-component planning resource directly in [30]-[35]. In fact, the management risk and the overall cost of electricity utilities can be reduced with the capacity cost prepaid to the long-term DR resource procured in the ADN planning phase [36]. For example, both PJM capacity market, called the reliability pricing model, and ISO-NE forward capacity market (FCM) procure DR resources to meet anticipated demands on a rolling three-year schedule [37]. In this paper, both the short-time-scale dispatching of DR and the long-time-scale procurement of DR resources are considered in the ADN planning to improve the benefits of electricity utilities.

In this paper, a novel bi-level coordinated ADN planning model is presented, considering DR resources and severely restricted scenarios (SRSs) screened out by a shadow-price-based scenario screening method. The main contributions of this paper are as follows.

1) The DR resource is regarded as a non-component planning resource and integrated into the proposed bi-level coordinated ADN planning model, considering both the capacity cost prepaid in the planning phase and the energy cost calculated in the operation phase. A better trade-off between long-term investment cost and short-term operation cost is achieved by the proposed model with DR resources than the models without DR resources.

2) Based on the shadow price theory in power system economics, the scenario impact factor is presented to evaluate the economic benefits of ADN resource planning in each scenario, which effectively reflects the influence of the ADN operation scenario on the ADN planning. The screening of massive scenarios for ADN planning is efficiently achieved to select out the important SRSs to be planned, which helps obtain better planning results than the methods with experiential predetermined scenarios.

II. DR in ADN Planning and Operation

Figure 1 illustrates the coordinated optimization of ADN. Generally, the long-term and ultra-short-term load demands in ADN are met with the investment and the economic dispatch of component resources such as lines and ESSs, respectively. Due to the high penetration of DG, ADN planners need to consider the short-term or even ultra-short-term load demands under various operation scenarios and achieve a coordinated optimization of the ADN planning and operation. The short time-scale operation cost can be reduced by avoiding load curtailment and consuming more renewable energy through the dispatch of ESS. However, due to its long lifecycle and high construction cost, the ESS configuration cannot be changed flexibly. As a non-component planning resource, the DR contract is signed by power consumers with electricity utilities, which is characterized by low capacity price, high energy price and short contract term [38]. For example, the ISO-NE annual capacity auction prices are only 4.63 \$/(kW·month) and 3.80 \$/(kW·month), in 2018 and 2019, respectively. Within the DR contract period, customers participating in capacity market receive payments for the load (e.g., air conditioners [39], water heaters [40], and ice-storage air-conditioners [41]) reductions, which are made to satisfy the short-term dispatch demand [42], effectively delaying the construction of lines and ESSs. When the contract expires, the DR contract will not be renewed if the controllable load is no longer required for the economic dispatch. Consequently, less long-term impacts on the ADN and better economic benefits to deal with the short-term dispatch demand are achieved through the procurement of DR resources compared with the construction of component planning resources such as lines and ESSs in some situations.

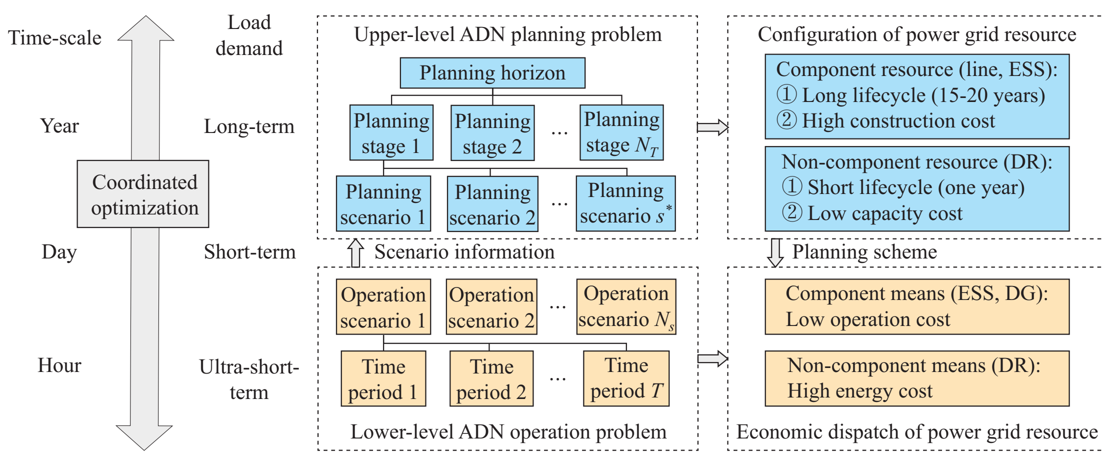

Fig. 1. Coordinated optimization of ADN.

In the ADN planning phase, the DR capacity cost C^{cap} is paid by electricity utilities to DR resource providers, i.e.,

$$C^{cap}=\sum_{n=1}^{N_T}(1+\rho)^{-n+1}\sum_{m\in\Omega_m}\sum_{i\in\Omega_{node}^m}c_{n,m,i}^{cap}P_{n,m,i}^{cap} \tag{1}$$

Based on the characteristics of different DR resources and consumer psychology, the maximum potential coefficient $\alpha_{n,m,i}^{DR}$ reflects the largest incentive-based response capacity of the DR resource provider at node i of load type m at planning stage n. The contract capacity $P_{n,m,i}^{cap}$ is limited by $\alpha_{n,m,i}^{DR}$, which is expressed as:

$$0\le P_{n,m,i}^{cap}\le \bar{P}_{n,m,i}^{load}\alpha_{n,m,i}^{DR} \tag{2}$$

The piecewise linear curve of $\alpha_{n,m,i}^{DR}$ represented in Fig. 2 is expressed as:

$$\alpha_{n,m,i}^{DR}=\begin{cases}0 & 0\le c_{n,m,i}^{cap}\le c_{n,m,dead}^{cap}\\ K_{n,m}^{DR}(c_{n,m,i}^{cap}-c_{n,m,dead}^{cap}) & c_{n,m,dead}^{cap}<c_{n,m,i}^{cap}<c_{n,m,sat}^{cap}\\ \alpha_{n,m,\max}^{DR} & c_{n,m,i}^{cap}\ge c_{n,m,sat}^{cap}\end{cases} \tag{3}$$

In the ADN operation phase, the procured DR resources can be dispatched for economic operation in all scenarios. The DR energy cost C_s^{ene} is calculated according to the actual usage of DR resources in scenario s, i.e.,

$$C_s^{ene}=\sum_{m\in\Omega_m}\sum_{i\in\Omega_{node}^m}\sum_{t=t_{m,i}^{start}}^{t_{m,i}^{end}}c_{n,m,i}^{ene}P_{s,m,i,t}^{DR}\Delta t \tag{4}$$

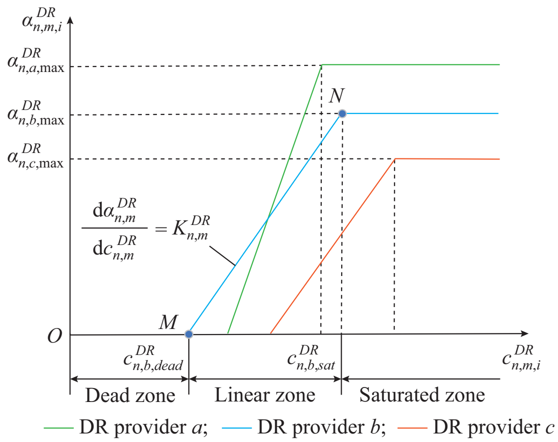

Fig. 2. Piecewise linear curves of the maximum potential coefficient.

For each operation scenario s, the hourly DR power is constrained by the minimum limit and the contract capacity during the DR event period, as shown in (5); and the hourly DR power is zero beyond the DR event period, as shown in (6); and the duration of each DR event period cannot exceed the maximum limit, as shown in (7).

$$P_{n,m,\min}^{DR} \le P_{s,m,i,t}^{DR} \le P_{n,m,i}^{cap} \quad \forall t \in \left[t_{m,i}^{start}, t_{m,i}^{end}\right] \tag{5}$$

$$P_{s,m,i,t}^{DR} = 0 \quad \forall t \notin \left[t_{m,i}^{start}, t_{m,i}^{end}\right] \tag{6}$$

$$t_{m,i}^{end} - t_{m,i}^{start} \le T_{\max}^{DR} \tag{7}$$

III. Bi-level Coordinated ADN Planning Model Considering DR Resource and SRS

Generally, the best economics of the ADN planning scheme is guaranteed in the planning model based on a universal operation scenario set. However, the number of decision variables and constraints is too large to be solved within an acceptable time. A planning scenario set with finite predetermined scenarios may lead to incorrect planning decisions. Ignoring some representative scenarios could lead to the inadequate investment cost and high operation cost; and over-evaluating the risks of some scenarios might lead to low utilization for the newly installed components and high investment cost. To reach an acceptable optimization time and achieve a trade-off between the investment cost and the operation cost during the whole planning period, an SRS set is built through scenario screening for the bi-level coordinated ADN planning model in this paper. The non-network solution, including the economic dispatch strategies and the restricted degrees of scenarios, is obtained in the lower level of the proposed model. Then, the SRSs are screened out and fed back to the upper level of the model to obtain the network solution. The approximately optimal solution is obtained after several iterations between the two levels.

A. Economic Dispatch Problem of ADN Considering DR in Lower Level

As discussed in Section II, the ability of ADN to deal with short-term operation risks caused by the mass connection of DG can be enhanced by DR, which is considered in the economic dispatch problem in the lower level of the model.

In the lower level of the proposed model, the decision variables include the hourly power of ESS, DR, WT, PV, and load shedding. The economic dispatch problem is to minimize the daily operation cost C_s^{ope}, which includes the energy purchase cost C_s^{pur}, power loss cost C_s^{loss}, DR energy cost C_s^{ene}, and penalty cost $C_s^{penalty}$ for PV curtailment, WT curtailment, and load shedding, and is expressed as:

$$\min C_s^{ope} = C_s^{pur} + C_s^{loss} + C_s^{ene} + C_s^{penalty} \tag{8}$$

$$C_s^{pur} = \sum_{i \in \Omega_{sub}} \sum_{t=1}^{T} P_{s,i,t}^{pur} c_t^{pur} \Delta t \tag{9}$$

$$C_s^{loss} = \sum_{ij \in \Omega_{line}} \sum_{t=1}^{T} c_t^{pur} P_{s,ij,t}^{loss} \Delta t = \sum_{ij \in \Omega_{line}} \sum_{t=1}^{T} c_t^{pur} I_{s,ij,t}^2 r_{ij} \Delta t \tag{10}$$

$$\begin{aligned} C_s^{penalty} = \sum_{i \in \Omega_{node}} \sum_{t=1}^{T} \Big[& c^{PVP} (\bar{P}_{s,i,t}^{PV} - P_{s,i,t}^{PV}) \Delta t + \\ & c^{WTP} (\bar{P}_{s,i,t}^{WT} - P_{s,i,t}^{WT}) \Delta t + c^{shed} P_{s,i,t}^{shed} \Delta t \Big] \end{aligned} \tag{11}$$

The decision variables of the economic dispatch problem are constrained by the DR constraints (5)-(7) and the operation constraints. The operation constraints are represented as:

$$(1-\theta_{WT}) \bar{P}_{s,i,t}^{WT} \le P_{s,i,t}^{WT} \le \bar{P}_{s,i,t}^{WT} \tag{12}$$

$$(1-\theta_{PV}) \bar{P}_{s,i,t}^{PV} \le P_{s,i,t}^{PV} \le \bar{P}_{s,i,t}^{PV} \tag{13}$$

$$\sum_{jk \in \Omega_{line}} P_{s,jk,t}^{line} = \sum_{ij \in \Omega_{line}} (P_{s,ij,t}^{line} - I_{s,ij,t}^2 r_{ij}) - P_{s,j,t} \tag{14}$$

$$\sum_{jk \in \Omega_{line}} Q_{s,jk,t}^{line} = \sum_{ij \in \Omega_{line}} (Q_{s,ij,t}^{line} - I_{s,ij,t}^2 \sigma_{ij}) - Q_{s,j,t} \tag{15}$$

$$P_{s,j,t} = \bar{P}_{s,j,t}^{load} - P_{s,j,t}^{pur} - P_{s,j,t}^{WT} - P_{s,j,t}^{PV} - P_{s,j,t}^{shed} - P_{s,j,t}^{DR} - P_{s,j,t}^{dis} + P_{s,j,t}^{char} \tag{16}$$

$$Q_{s,j,t} = Q_{s,j,t}^{load} - Q_{s,j,t}^{pur} - Q_{s,j,t}^{WT} - Q_{s,j,t}^{PV} + Q_{s,j,t}^{CB} \tag{17}$$

$$V_{s,i,t}^2 I_{s,ij,t}^2 = (P_{s,ij,t}^{line})^2 + (Q_{s,ij,t}^{line})^2 \tag{18}$$

$$\left| P_{s,ij,t}^{line} \right| \le S_{n,ij}^{line} \tag{19}$$

$$P_{s,j,t}^{pur} \ge 0 \tag{20}$$

$$V_{s,j,t}^2 \le V_{s,i,t}^2 - 2(r_{ij} P_{s,ij,t}^{line} + \sigma_{ij} Q_{s,ij,t}^{line}) + I_{s,ij,t}^2 (r_{ij}^2 + \sigma_{ij}^2) + M(1 - y_{n,ij}^{line}) \tag{21}$$

$$V_{s,j,t}^2 \ge V_{s,i,t}^2 - 2(r_{ij} P_{s,ij,t}^{line} + \sigma_{ij} Q_{s,ij,t}^{line}) + I_{s,ij,t}^2 (r_{ij}^2 + \sigma_{ij}^2) - M(1 - y_{n,ij}^{line}) \tag{22}$$

$$V_{i,\min} \le V_{s,i,t} \le V_{i,\max} \tag{23}$$

$$0 \le P_{s,i,t}^{shed} \le \lambda \bar{P}_{s,i,t}^{load} \tag{24}$$

$$0 \le x_{s,i,t}^{dis} + x_{s,i,t}^{char} \le 1 \tag{25}$$

$$\left| x_{s,i,t}^{dis} P_{s,i,t}^{dis} - x_{s,i,t}^{char} P_{s,i,t}^{char} \right| \le P_i^{ESS} \tag{26}$$

$$E_{i,\min}^{SOC} \le E_{s,i,t}^{SOC} \le E_{i,\max}^{SOC} \tag{27}$$

$$E_{s,i,t}^{SOC} = (1-\varepsilon) E_{s,i,t-1}^{SOC} - \frac{1}{\gamma_{dis}} P_{s,i,t}^{dis} \Delta t + \gamma_{ch} P_{s,i,t}^{ch} \Delta t \tag{28}$$

$$E_{s,i,1}^{SOC} = E_{s,i,T}^{SOC} \tag{29}$$

The hourly output power of DGs is constrained in (12) and (13). The nodal power balance equations are represented in (14)-(17). The square of the current magnitude of line ij is computed in (18). The power flow constraint considering the bidirectional power flow is formulated in (19). Constraint (20) prevents power from being injected into the upper power grid. The big-M method is used in (21) and (22) to deal with the nonlinear terms when considering the radial topology distribution network [43], [44]. The nodal voltage is limited in (23). The load shedding power of every node is constrained in (24). The constraints for discharging and charging status and hourly power of ESS are defined in (25) and (26), respectively. The stored energy of ESS is constrained in (27). The ESS power balance constraint is shown in (28). Constraint (29) guarantees the conservation of daily charging and discharging energy.

B. ADN Planning Considering DR Resource in Upper Level

The objective of the ADN planning model is to minimize the total cost C_{total} including the investment cost of lines and ESSs C_{line}^{inv} and C_{ESS}^{inv}, the capacity cost of DR contract C^{cap}, the maintenance costs of lines and ESSs C_{line}^{m} and C_{ESS}^{m}, and the daily economic dispatching cost under SRSs C_{s*}, which is formulated as:

$$\min C_{total} = C_{line}^{inv} + C_{ESS}^{inv} + C^{cap} + C_{line}^{m} + C_{ESS}^{m} + C_{s*} \tag{30}$$

$$C_{line}^{inv} = \sum_{n=1}^{N_T} \frac{(1+\rho)^{-n}}{\rho} \frac{\rho(1+\rho)^{Y^{line}}}{(1+\rho)^{Y^{line}}-1} \left(\sum_{ij \in \Omega_{Nline}} \sum_{r \in \Omega_{Nlr}} x_{n,ij}^{line} c_r L_{ij} + \sum_{ij \in \Omega_{Rline}} \sum_{r \in \Omega_{Rlr}} x_{n,ij}^{line} c_r L_{ij} \right) \tag{31}$$

$$C_{ESS}^{inv} = \sum_{n=1}^{N_T} \frac{(1+\rho)^{-n}}{\rho} \frac{\rho(1+\rho)^{Y^{ESS}}}{(1+\rho)^{Y^{ESS}}-1} \left[\sum_{i \in \Omega_{NESS}} x_{n,i}^{NESS} c_{S,i}^{NESS} + \sum_{i \in \Omega_{EESS} \cup \Omega_{NESS}} \left(c_{P,i}^{ESS} P_{n,i}^{ESS} + c_{E,i}^{ESS} E_{n,i}^{ESS} \right) \right] \tag{32}$$

$$C_{line}^{m} = \sum_{n=1}^{N_T} (1+\rho)^{-n} \left(\sum_{ij \in \Omega_{Eline}} c_{line}^{m} L_{ij} + \sum_{ij \in \Omega_{Nline}} x_{n,ij}^{line} c_{line}^{m} L_{ij} \right) \tag{33}$$

$$C_{ESS}^{m} = \sum_{n=1}^{N_T} (1+\rho)^{-n} \sum_{i \in \Omega_{EESS} \cup \Omega_{NESS}} c_{ESS}^{m} E_{n,i}^{ESS} \tag{34}$$

$$C_{s*} = \sum_{s \in \Omega_{s*}} \delta (1+\rho)^{-n} p_s C_s^{ope} \tag{35}$$

In (30)-(35), the long-term decision variables include investment variables for the installation and reinforcement of lines $x_{n,ij}^{line}$, the installation and expansion of ESS $x_{n,i}^{NESS}$, $P_{n,i}^{ESS}$ and $E_{n,i}^{ESS}$ and the contract amount of DR $P_{n,m,i}^{cap}$. The investment constraints are represented as:

$$\sum_{n=1}^{N_T} x_{n,ij}^{line} \le 1 \tag{36}$$

$$\sum_{n=1}^{N_T} x_{n,i}^{NESS} \le 1 \tag{37}$$

$$0 \le P_{n,i}^{ESS} \le P_{i,\max}^{ESS} \tag{38}$$

$$0 \le E_{n,i}^{ESS} \le E_{i,\max}^{ESS} \tag{39}$$

$$y_{n,ij}^{line} = \begin{cases} 1 & ij \in \Omega_{Eline} \\ \sum_{n=1}^{N_T} x_{n,ij}^{line} & ij \in \Omega_{Nline} \end{cases} \tag{40}$$

$$\sum_{ij \in \Omega_{Lline} \cap \Omega_{Eline}} y_{n,ij}^{line} + \sum_{ij \in \Omega_{Lline} \cap \Omega_{Nline}} y_{n,ij}^{line} \le N_{LS} - 1 \tag{41}$$

$$C_n^{inv} \le C_{\max}^{inv} \tag{42}$$

Throughout the entire planning horizon, each line and ESS are allowed to be constructed once at most, as constrained in (36) and (37), respectively. The maximum power and stored energy limit of ESS are constrained in (38) and (39), respectively. The construction state of line is constrained in (40). The radiality of the distribution network is constrained in (41). As discussed in Section II, DR potential capability is constrained in (2). The investment cost constraint at every planning stage is represented in (42).

The constraints associated with the ADN operation should be satisfied at each time period in all planning scenarios, which are listed in (12)-(29).

C. Shadow-price-based SRS Screening Method

The uncertainty and fluctuation levels of the ADN are enhanced by the development of DG and load, which generates a variety of restricted scenarios. The restricted scenarios represent those with congestion and high operation cost due to the insufficiency capacity of power grid resources. The best planning scheme can be achieved with the planning model considering all operation scenarios but is time-consuming and difficult to be solved. There are unrestricted scenarios and some restricted scenarios that do not need to be considered in the planning phase because of their low restricted degrees or probabilities. The operation risks in these scenarios may be reduced when the network solution is made for other scenarios with more severely restricted degrees. In this paper, a novel shadow-price-based SRS screening method is proposed to screen out the correct scenarios, which should be considered in ADN planning in the massive operation scenarios.

The shadow price, i.e., Lagrange multiplier, is the additional product when using the primal-dual interior-point method based on Karush-Kuhn-Tucker (KKT) conditions, which evaluates the worth of increment for additional unit capacity quantitatively [45]. In the ADN planning model, the limits of some constraints are decided by the capacities of power system resources. The Lagrange multipliers of the upper limit of DR power constraint, the upper and lower limits of power flow constraint, and the upper limits of ESS power and stored energy constraints (i.e., $\mu_{s,m,i,t}$, $v_{s,ij,t}^{u}$, $v_{s,ij,t}^{d}$, $\pi_{s,j,t}$, and $\tau_{s,j,t}$) correspond to the shadow prices of DR resources, lines and ESSs, respectively. Based on these Lagrange multipliers, a new factor named as the shadow price of scenario Ψ_s is defined to evaluate the restricted degree of scenario, which is represented as:

$$\Psi_s = \sum_{m \in \Omega_m} \sum_{i \in \Omega_{node}^{m}} \sum_{t=1}^{T} \frac{\mu_{s,m,i,t}}{c_m^{cap}} + \sum_{ij \in \Omega_{Nline} \cup \Omega_{Eline}} \sum_{t=1}^{T} \frac{v_{s,ij,t}^{u} + v_{s,ij,t}^{d}}{c_r} + \sum_{i \in \Omega_{EESS} \cup \Omega_{NESS}} \sum_{t=1}^{T} \left(\frac{\pi_{s,i,t}}{c_{P,i}^{ESS}} + \frac{\tau_{s,i,t}}{c_{E,i}^{ESS}} \right) \tag{43}$$

It is noted that the scenario probability is independent of the shadow price of scenario, which is important to evaluate the restricted degree of scenario. The scenario impact factor ζ_s is defined to describe the restricted degree of scenario and screen out the SRSs, and it can be represented as:

$$\zeta_s = \Psi_s p_s \tag{44}$$

The overall scarcity of the ADN resources in operation scenario s is reflected through the scenario impact factor ζ_s. Unit investment in the scenario with a larger ζ_s will get better marginal benefits in reducing the operation costs and risks. According to the impact factor ζ_s, all operation scenarios are evaluated objectively and those with great marginal benefits of investment are selected into the SRS set Ω_{s*} for ADN planning, which can be represented as:

$$\Omega_{s*} = \left\{ s* \left| \zeta_{s*} \geq \max\left\{ \zeta_0, \frac{1}{N_s} \sum_{s \in \Omega_s} \zeta_s \right\}, s* \in \Omega_s \right. \right\} \tag{45}$$

According to (45), the scenarios with larger impact factors than the threshold or the average of all scenario impact factors ζ_0 are included in the SRS set (i.e., the planning scenario set). The SRS set simulates the information transmitted from system operators to ADN planners.

D. Bi-Level Coordinated ADN Planning Model

1) Upper-level Model

$$\begin{cases} \min\limits_{\Omega_u} C_{total} = C_{line}^{inv} + C_{line}^{inv} + C^{cap} + C_{line}^{m} + C_{ESS}^{m} + C_{s*} \\ \text{s.t. } (2), (5)\text{-}(7), (12)\text{-}(29), (36)\text{-}(42) \\ \qquad \forall s \in \Omega_{s*}, \forall m \in \Omega_{node}^{m}, \forall i \in \Omega_{node}, j \in \Omega_{node}, k \in \Omega_{node}, \\ \qquad \forall ij \in \Omega_{line}, jk \in \Omega_{line}, \forall n = 1, 2, ..., N_T, \forall t = 1, 2, ..., T \end{cases} \tag{46}$$

2) Lower-level Model

$$\begin{cases} \min\limits_{\Omega_l} C_s^{ope} = C_s^{pur} + C_s^{loss} + C_s^{ene} + C_s^{penalty} \\ \text{s.t. } (5)\text{-}(7), (12)\text{-}(29) \\ \qquad \forall s \in \Omega_s, \forall m \in \Omega_{node}^{m}, \forall i \in \Omega_{node}, j \in \Omega_{node}, k \in \Omega_{node}, \\ \qquad \forall ij \in \Omega_{line}, jk \in \Omega_{line}, \forall t = 1, 2, ..., T \end{cases} \tag{47}$$

The proposed bi-level planning model consists of a master problem of ADN planning and a set of sub-problems of ADN operation. The intermediate variables between the upper- and lower-level models are the SRSs screened out based on the simulation result of ADN operation and the ADN planning solution, which reflects the interaction between ADN planning and operation.

IV. Iterative Solving Process of Bi-level Coordinated Planning Model

With the SRS screening method introduced in Section III-C, the planning scenario sets are built for the planning model to obtain the network solutions in every iteration until the approximately optimal solution is obtained. In the solving process, the second-order cone relaxation is applied to simplify the non-convex nonlinear planning model in the lower level to the convex linear planning model [46]-[48].

A. Iterative Solving Process of Bi-level Optimization Model

The flowchart of the proposed bi-level coordinated planning model is presented in Fig. 3. The iterative solving steps are summarized as follows.

Step 1: input the initial distribution network information (network solution) and the parameters for ADN planning.

Step 2: set $\tau = 0$ and $s = 1$.

Step 3: solve the lower-level economic dispatch in scenario s. The non-network solution including the economic daily dispatch strategy and the Lagrange multipliers (i.e., shadow prices) of DGs, ESSs, and DR contracts is obtained.

Step 4: calculate Ψ_s and ζ_s.

Step 5: if $s > N_s$, turn to *Step 6*; otherwise, set $s = s + 1$ and return to *Step 3*.

Step 6: screen out Ω_{s*} with the proposed SRS screening method.

Step 7: if Ω_{s*} is an empty set, turn to *Step 11*; otherwise, return to *Step 8*.

Step 8: solve the upper-level planning problem considering Ω_{s*}. The τ^{th} network solution including the line and ESS investment and the DR contract signing decisions is obtained.

Step 9: if the planning result is changed, turn to *Step 10*; otherwise, turn to *Step 11*.

Step 10: update the distribution network scheme with the network solution and set $\tau = \tau + 1$.

Step 11: output the ADN planning result.

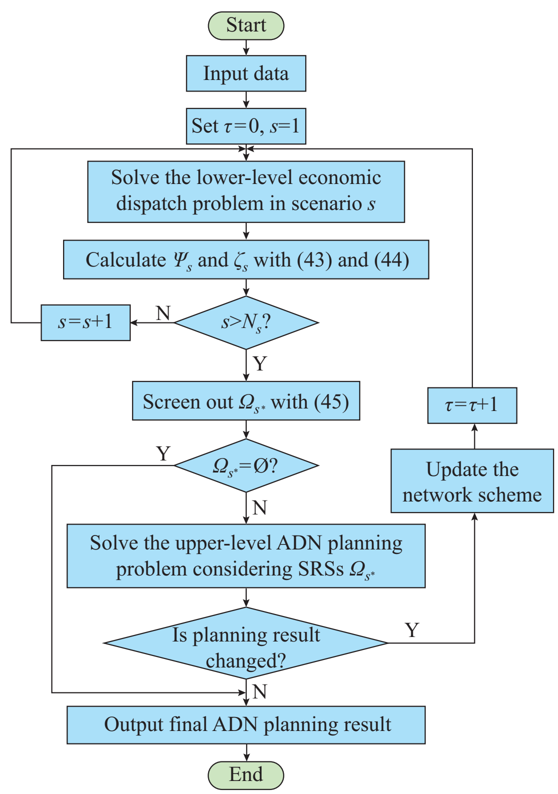

Fig. 3. Flowchart of proposed bi-level coordinated planning model.

B. Conversion Method of Constraint Based on Second-order Cone Relaxation

The proposed economic dispatch problem is a non-convex nonlinear programming problem which is difficult to solve. The second-order cone relaxation can guarantee the accuracy of the solution algorithm and meet the computational speed requirement [49]. Using the conversion equations (48) and (49), (14), (15), (18), and (21)-(23) are reformulated to (50)-(55). Then, (52) is converted to (56) by using second-order cone relaxation. In the upper level, the mixed-integer conic quadratic (MICQ) model is converted to the mixed-integer linear planning (MILP) model. The approximately optimal solutions of the upper-level and lower-level models are obtained by the commercial solver CPLEX [50]-[52].

$$I^{\varphi}_{s,ij,t} = I^{2}_{s,ij,t} \tag{48}$$

$$V^{\varphi}_{s,i,t} = V^{2}_{s,i,t} \tag{49}$$

$$\sum_{jk \in \Omega_{line}} P^{line}_{s,jk,t} = \sum_{ij \in \Omega_{line}} (P^{line}_{s,ij,t} - I^{\varphi}_{s,ij,t} r_{ij}) - P_{s,j,t} \tag{50}$$

$$\sum_{jk \in \Omega_{line}} Q^{line}_{s,jk,t} = \sum_{ij \in \Omega_{line}} (Q^{line}_{s,ij,t} - I^{\varphi}_{s,ij,t} \sigma_{ij}) - Q_{s,j,t} \tag{51}$$

$$V^{\varphi}_{s,i,t} I^{\varphi}_{s,ij,t} = (P^{line}_{s,ij,t})^2 + (Q^{line}_{s,ij,t})^2 \tag{52}$$

$$V^{\varphi}_{s,j,t} < V^{\varphi}_{s,i,t} - 2(r_{ij} P^{line}_{s,ij,t} + \sigma_{ij} Q^{line}_{s,ij,t}) + I^{\varphi}_{s,ij,t}(r^2_{ij} + \sigma^2_{ij}) + M(1 - y^{line}_{n,ij}) \tag{53}$$

$$V^{\varphi}_{s,j,t} \geq V^{\varphi}_{s,i,t} - 2(r_{ij} P^{line}_{s,ij,t} + \sigma_{ij} Q^{line}_{s,ij,t}) + I^{\varphi}_{s,ij,t}(r^2_{ij} + \sigma^2_{ij}) - M(1 - y^{line}_{n,ij}) \tag{54}$$

$$V^{2}_{i,\min} \leq V^{\varphi}_{s,i,t} \leq V^{2}_{i,\max} \tag{55}$$

$$\left\| \begin{matrix} 2P^{line}_{s,ij,t} \\ 2Q^{line}_{s,ij,t} \\ I^{\varphi}_{s,ij,t} - V^{\varphi}_{s,i,t} \end{matrix} \right\|_2 \leq I^{\varphi}_{s,ij,t} + V^{\varphi}_{s,i,t} \tag{56}$$

where $\|\cdot\|_2$ represents the Euclidean L2-norm.

V. Case Study

A 62-node distribution system in Jianshan New District, Zhejiang Province, China, as shown in Fig. 4, is used to illustrate the effectiveness of the proposed model.

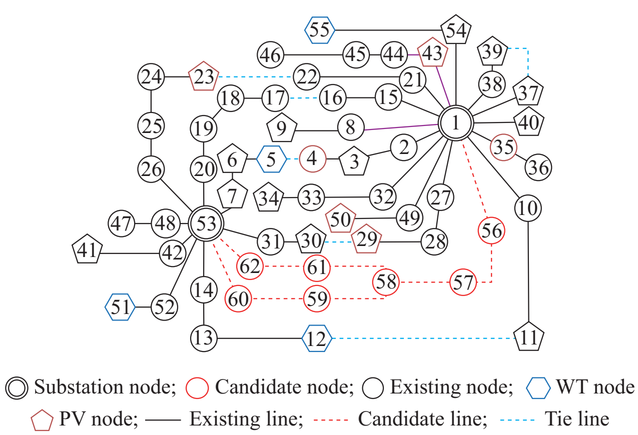

Fig. 4. Initial network topology of an actual 62-node distribution system.

The distribution system comprises two substation nodes, 55 industrial load nodes, five commercial load nodes, and 62 lines. The planning problem is divided into four planning stages, and each stage represents a period of one year. The candidate nodes for ESS and DR contract, the location and capacity information of DGs, and the parameters of the planning model are shown in Tables I-III, respectively. The PV and WF scenarios are clusted into six and three scenarios, respectively,and shown in Fig. 5. A universal operation scenario set with 144 joint scenarios is considered for scenario screening. The probability of the joint scenario is the product of the probabilities of PV, WT, and load.

TABLE I
Candidate Nodes For ESS and DR Contract

Type	No. of node
ESS	5, 8, 9, 10, 12, 13, 14, 23, 33, 34, 35, 39, 40, 41, 54, 55, 56
DR contract	5, 6, 8, 9, 12, 13, 14, 39, 41, 51, 55

TABLE II
Location and Capacity Information of DG

Type	No. of node	Maximum output power (MW)
PV	4	1.3
	23	2.0
	29	2.7
	35	2.7
	43	1.8
	50	1.2
WT	5	3.6
	12	2.1
	55	4.6

TABLE III
Parameters of Planning Model

Type	Parameter	Value
ESS	Fixed construction cost	¥10000
	Unit rated power cost	300000 ¥/MW
	Unit capacity cost	300000 ¥/MWh
	Maintenance cost	10000 ¥/(MWh·year)
	Lifecycle	15 year
Line	Maintenance cost	2000 ¥/(km·year)
	Lifecycle	20 year
	Unit investment cost (JKLYJ-20-240)	¥700000
	Impedance (JKLYJ-20-240)	(0.13+j0.34)Ω/km
	Maximum capacity (JKLYJ-20-240)	8.6 MW
	Unit investment cost (JKLYJ-20-300)	¥800000
	Impedance (JKLYJ-20-300)	(0.16+j0.29)Ω/km
	Maximum capacity (JKLYJ-20-300)	10.6 MW
Operation	Unit penalty for load shedding	8000 ¥/MWh
	Unit penalty for PV and WT curtailment	4000 ¥/MWh
	Operation time of DSM	10:00 to 16:00
	Limit for nodal voltage	$[0.95V_B, 1.05V_B]$
Planning	Discount rate	8%
	Load growth rate	5%
	DG growth rate	7%
	Investment limit	¥3000000

Simulations have been implemented on a PC with an Intel Core i5 CPU at 1.8 GHz and 8 GB of RAM using the YALMIP tool in MATLAB and calculated with CPLEX 12.6. The termination for the branch-and-cut algorithm of CPLEX is set at an optimal gap tolerance equal to 0.01%.

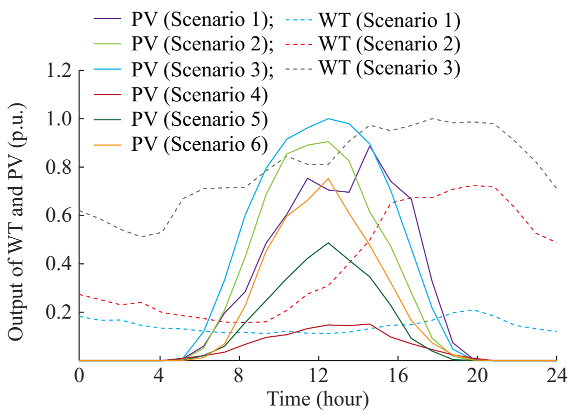

Fig. 5. Typical output curves of WT and PV.

A. Result of Proposed Bi-level Coordinated Planning

The final planning scheme and target distribution network topology of the proposed bi-level coordinated planning model considering DR resources and SRSs (BCP-DR-SRS model) are presented in Fig. 6 and Table IV, respectively. In Fig. 6 and Table IV, to meet the periodic growth of load in the ADN, $L_{1\text{-}56}$, $L_{60\text{-}57}$, $L_{53\text{-}61}$, and $L_{53\text{-}60}$ are newly installed; $L_{53\text{-}14}$, $L_{1\text{-}43}$, $L_{1\text{-}8}$, $L_{53\text{-}26}$, and $L_{43\text{-}44}$ are reinforced; ESSs with different rated power and capacities are newly installed at nodes 5, 10, 23, and 39; and DR contracts are signed with users at nodes 9 (i.e., 45 kW) at planning stage 1, at nodes 38 and 39 (i.e., 80 kW and 14 kW, respectively) at planning stage 2, and at nodes 38 and 39 (i.e., 170 kW and 152 kW, respectively) at planning stage 3.

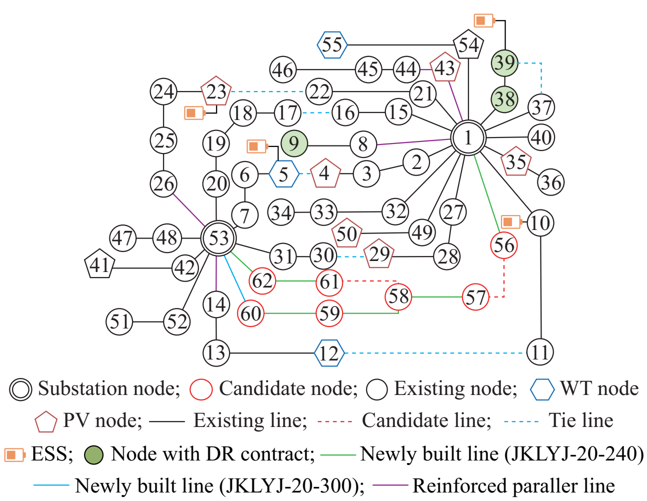

Fig. 6. Target distribution network topology of BCP-DR-SRS model.

In order to demonstrate the effectiveness of the proposed SRS screening method, the restricted degrees of six scenarios out of all SRSs are presented in Table V. Both the typical scenarios (e.g., scenarios 103, 104, 139, and 140) with probabilities larger than 7.0% and the extreme scenarios (e.g., scenarios 109 and 113) with probabilities less than 2% are included in the SRS set. Under these SRSs, the loads at nodes 9, 12, 23, 39, and 46 are shed for the power flowing through $L_{1\text{-}8}$, $L_{53\text{-}14}$, $L_{53\text{-}26}$, $L_{1\text{-}38}$, and $L_{1\text{-}44}$, which exceeds the maximum capacity limits. On the other hand, the shadow price of scenario 113 (Ψ_{113}) is 2064.2, which is higher than those of scenarios 140 and 139 ($\Psi_{140}=483.9$, $\Psi_{139}=474.8$).

TABLE IV
PLANNING SCHEME OF BCP-DR-SRS MODEL

Planning stage	Line	Newly installed ESS	Rated power of ESS (MW)	Rated capacity of ESS (MWh)	DR	Capacity of DR (kW)
1	$L^R_{53\text{-}14}$,$L^R_{1\text{-}43}$, $L^A_{1\text{-}56}$,$L^A_{60\text{-}57}$, $L^A_{53\text{-}61}$,$L^B_{53\text{-}60}$	ESS_5	0.4	0.7	DR_9	45
		ESS_{10}	0.8	1.5		
		ESS_{23}	1.4	2.8		
		ESS_{39}	1.2	2.4		
2	$L^R_{1\text{-}8}$	ESS_5	0.4	0.8		
		ESS_{10}	0.5	1.0		
		ESS_{23}	0.6	2.5		
		ESS_{39}	0.8	1.6		
3	$L^R_{53\text{-}26}$,$L^R_{43\text{-}44}$				DR_{38}	80
					DR_{39}	14
4					DR_{38}	170
					DR_{39}	152

Note: the superscript "R" represents newly reinforced parallel lines; the superscripts "A" and "B" represent two types of newly built lines, i.e., JKLYJ-20-240 and JKLYJ-20-300.

TABLE V
RESTRICTED DEGREES OF SRSS BEFORE AND AFTER PLANNING

Scenario (planning stage)	Scenario probability p_s (%)	Shadow price of scenario Ψ_s		Scenario impact factor ζ_s	
		Before planning	After planning	Before planning	After planning
140 (4)	8.0	483.9	113.6	38.7	9.1
139 (4)	8.0	474.8	113.6	38.0	9.1
104 (3)	8.0	432.2	84.0	34.6	6.7
103 (3)	8.0	413.2	84.0	33.1	6.7
109 (4)	1.5	1753.9	1129.6	26.3	16.9
113 (4)	1.2	2064.2	1883.0	24.8	22.6

However, scenario 113 is not included in the SRS set at first because it has a low probability ($p_{113}=1.2\%$) which makes its scenario impact factor ($\zeta_{113}=24.8$) less than those of scenarios 140 ($\zeta_{140}=38.7$) and 139 ($\zeta_{139}=38.0$). After the first iteration of planning, the impact factors of scenarios 140 and 139 ($\zeta_{140}=8.78$, $\zeta_{139}=8.79$) decrease and are less than that of scenario 113 ($\zeta_{113}=23.4$). Then, scenario 113 is included in the SRS set which influences the planning result in the second iteration. The original and final scenario impact factors of all operation scenarios are presented in Fig. 7, where all scenario impact factors decrease after planning, indicating that the shortages of network resources in all operation scenarios are alleviated. The scenario impact factors of scenarios 140, 139, 109, and 113 decrease by 76.5%, 76.1%, 35.6%, and 8.8%, respectively, indicating that the ADN operation risks are effectively reduced through the proposed BCP-DR-SRS model. In sum, the restricted degrees of scenarios are objectively quantized by the scenario impact factors to effectively solve various restricted operation problems in the ADN planning.

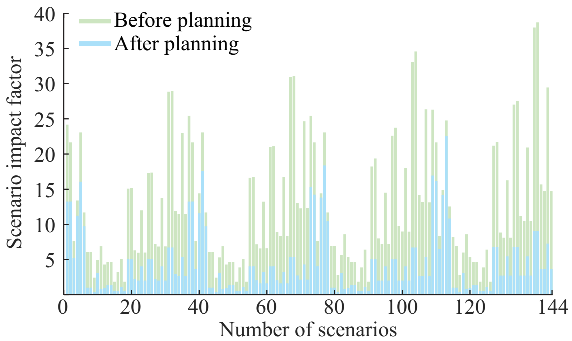

Fig. 7. Scenario impact factors before and after planning.

To demonstrate the DG consumption ability of the ADN optimized by BCP-DR-SRS model, the DG consumption before and after planning is compared in Fig. 8. In Fig. 8, the actual output curves of WT and PV after planning are higher than those before planning, indicating a higher renewable energy consumption in the target ADN. Considering all scenarios, the average WT and PV consumption rates increase from 80.3% and 95.7% to 96.1% and 99.2%, respectively.

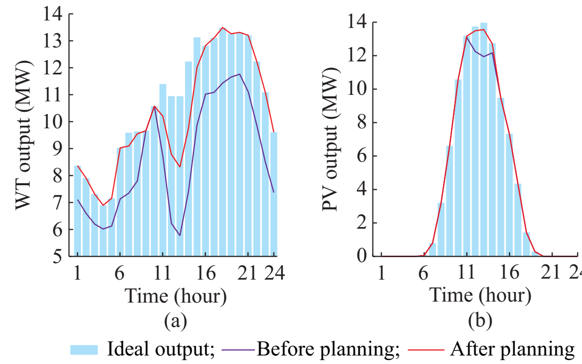

Fig. 8. Ideal and actual output curves of WT and PV in scenario 109. (a) WT. (b) PV.

B. Comparison with Other Models

To illustrate the advantages of the proposed BCP-DR-SRS model, other models are presented for comparison, i. e., bi-level coordinated planning model considering SRSs (BCP-SRS model), single-level planning model considering multi-scenario technique [53] (SP-MT model) and single-level planning model considering DR resources and multi-scenario technique (SP-DR-MT model). According to [53], the planning scenarios consist of four kinds of typical scenarios and one kind of extreme scenario at each planning stage provided by system operators, which are described with scenarios 24, 27, 31, 32, 35, 60, 63, 67, 68, 71, 96, 99, 103, 104, 107, 132, 135, 139, 140, and 143 in SP-MT and SP-DR-MT models. The planning schemes of BCP-STS, SP-MT and SP-DR-MT models are presented in Table VI.

TABLE VI
PLANNING SCHEMES OF BCP-SRS, SP-MT AND SP-DR-MT MODELS

Planning stage	BCP-SRS				Line in SP-MT [53]	SP-DR-MT		
	Line	Newly installed ESS	Rated power of ESS (MW)	Rated capacity of ESS (MWh)		Line	DR	Capacity of DR (kW)
1	$L^R_{1\text{-}8}$, $L^R_{53\text{-}14}$, $L^R_{1\text{-}43}$, $L^A_{1\text{-}56}$, $L^A_{53\text{-}61}$, $L^B_{53\text{-}60}$	ESS_5 ESS_{23} ESS_{39} ESS_{54}	0.4 1.4 0.9 1.1	0.7 2.8 1.7 2.2	$L^R_{1\text{-}8}$, $L^R_{53\text{-}14}$, $L^R_{1\text{-}43}$, $L^A_{1\text{-}57}$, $L^A_{53\text{-}59}$, $L^A_{58\text{-}62}$, $L^R_{53\text{-}14}$	$L^R_{53\text{-}14}$, $L^R_{1\text{-}43}$, $L^A_{1\text{-}57}$, $L^A_{53\text{-}59}$, $L^A_{58\text{-}62}$, $L^B_{53\text{-}62}$	DR_9	36
2		ESS_5 ESS_{23} ESS_{39} ESS_{54}	0.4 0.6 0.4 0.9	0.8 2.5 0.8 1.8		$L^R_{1\text{-}8}$		
3	$L^R_{53\text{-}26}$, $L^R_{43\text{-}44}$				$L^R_{53\text{-}26}$, $L^R_{1\text{-}38}$, $L^R_{43\text{-}44}$	$L^R_{53\text{-}26}$, $L^R_{43\text{-}44}$	DR_{39}	74
4	$L^R_{1\text{-}38}$						DR_{39}	258

1) Effect of DR on ADN Considering Multi-time-scales

The hourly power of load, DRs, and nodal injection at bus 39 in scenario 139 in SP-DR-MT model is shown in Fig. 9. In the short time-scale, the peak load is controlled through DR, which reduces the annual operation cost. The investment costs of the four models are presented in Table VII. It can be seen that the operation cost in the target year (C^{ope}_{target}) of SP-DR-MT model is ¥1155000 less than that of SP-MT model, which proves the effectiveness of DR resources in avoiding load shedding in some short-term scenarios through dispatching the controlled load flexibly. In the long time-scale, the reinforcement of $L_{1\text{-}8}$ is delayed for one year and that of $L_{1\text{-}38}$ is canceled when comparing the planning scheme of SP-MT model with that of SP-DR-MT model in Table VI. In Table VII, the investment cost of lines and the total investment cost C^{inv} of SP-DR-MT model are ¥1773500 and ¥1742200 less than those of SP-MT model, respectively, which indicates the performance of DR resources in saving the investment cost. In sum, the better economic dispatch in the short time-scale and reduction of the investment cost in the long time-scale can be realized with DR resources effectively.

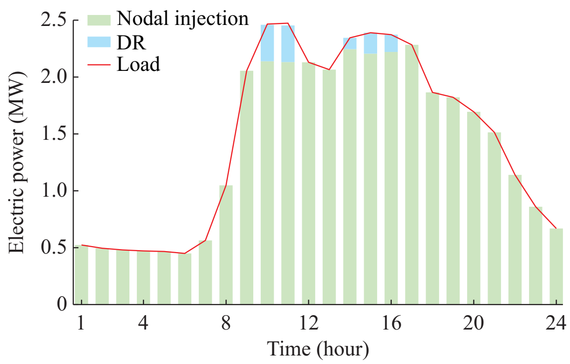

Fig. 9. Hourly power of load, DR, and nodal injection at bus 39 in scenario 139.

TABLE VII
COMPARISON OF INVESTMENT COSTS OF FOUR MODELS

Model	C_{line}^{inv} (¥10^7)	C_{ESS}^{inv} (¥10^7)	C^{cap} (¥10^4)	C_{line}^{m} (¥10^5)	C_{ESS}^{m} (¥10^5)	C_{target}^{ope} (¥10^8)	C^{inv} (¥10^7)
BCP-DR-SRS	1.22422	1.97789	4.56	1.068	4.217	1.092845	3.25952
BCP-SRS	1.38893	1.97789		1.153	4.217	1.092885	3.42052
SP-MT [53]	1.34468			1.165		1.361647	1.35633
SP-DR-MT	1.16733		4.56	1.022		1.350097	1.18211

2) Effect of SRS Screening Method on Cost and DG Consumption

The planning schemes of BCP-DR-SRS and SP-DR-MT models are compared to illustrate the effect of the proposed SRS screening method on investment and operation costs. It can be seen from Tables IV and VI that new ESSs at nodes 5, 23, 33, and 40 are not installed in the planning scheme of SP-DR-MT model because some scenarios with high risks (e.g., scenarios 109 and 113) are not considered in the planning phase. As shown in Table VII, the investment cost of SP-DR-MT model is ¥20774100 less than that of BCP-DR-SRS model; but the operation cost in the target year of SP-DR-MT model is ¥25725200 more than that of BCP-DR-SRS model. The different planning results of BCP-DR-SRS and SP-DR-MT models indicate that the determination of the planning scenario set has an obvious impact on the planning result, which further influences the operation cost of the ADN. As a result, the proposed SRS screening method can screen out the correct scenarios to achieve a better trade-off between the investment cost and the operation cost.

Figure 10 illustrates the operation cost difference between BCP-DR-SRS model and SP-DR-MT model in scenarios 1-6, 10-12, and 16, 17. In Fig. 10, the difference in scenario 17 is small and does not change much at planning stages. However, taking scenario 5 as an example, the difference of the operation cost increases stage by stage and reaches ¥54816 in the target year. BCP-DR-SRS model illustrates a better adaptability to the operation scenarios varying with the planning stages than the SP-DR-MT model.

In order to illustrate the effect of the SRS screening method on improving the DG consumption ability of the ADN, the penalty cost for WT and PV curtailment of four models are presented in Table VIII. In Table VIII, the penalty cost for WT and PV curtailment of BCP-SRS model is ¥3337300 less than that of SP-MT model during the whole planning period, which indicates that more renewable energy is efficiently consumed in the planned distribution network considering the scenarios screened out by the proposed SRS screening method.

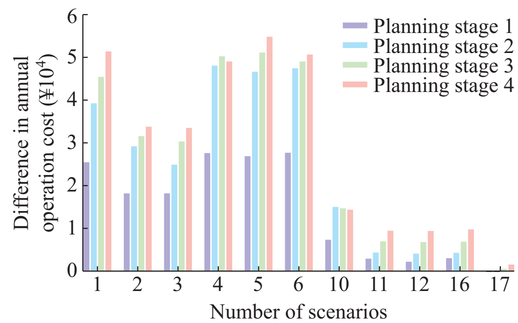

Fig. 10. Operation cost difference between BCP-DR-SRS model and SP-DR-MT model.

TABLE VIII
PENALTY COST FOR WT AND PV CURTAILMENT OF FOUR MODELS

Model	Penalty cost (¥)			
	Planning stage 1	Planning stage 2	Planning stage 3	Planning stage 4
BCP-DR-SRS	612500	527500	808200	1108500
BCP-SRS	614900	527500	813500	1126800
SP-MT	1128200	1367200	1758500	2166100
SP-DR-MT	1125400	1367200	1750900	2137600

In terms of computational burden, it is time-consuming to solve the planning model with the universal operation scenario set. The calculation time of the planning problem with BCP-DR-SRS model is 3 hours, which is acceptable for the distribution network planner in practice. In conclusion, the economic planning scheme can be achieved by the proposed BCP-DR-SRS model with the SRS screening method under an acceptable computation burden.

VI. CONCLUSION

In this paper, a bi-level coordinated planning model integrated with DR resources procurement and ESS/line configuration is proposed to deal with the increasing operation risks of the ADN. A shadow-price-based screening method is proposed to screen out the SRSs for ADN planning. With the coordinated optimization of the ADN operation and planning, the proposed model not only meets the long-term development demand of the distribution network, but also provides specific strategies for the short-term dispatch problem. Finally, the effectiveness of the proposed model is validated by the comparison between different ADN planning models based on an actual distribution system. The main conclusions are summarized as follows.

1) The proposed bi-level coordinated planning model, which regards DR as a new non-component means, can reduce the operation cost of the distribution network by dispatching the controllable load under SRSs in the short time-scale and delay the investment of the component planning resource by signing DR contracts in the long time-scale. Compared with component planning resources such as lines and ESSs, the non-component resource DR is configured more flexibly because of its low capacity price and short contract term. A better trade-off between the long-term investment cost and the short-term operation cost is obtained by the proposed model with DR resources in the ADN planning.

2) The proposed shadow price-based screening method effectively screens out SRSs for the ADN planning from a universal operation scenario set within an acceptable time. The DG consumption level of the distribution network is effectively improved by the proposed planning model considering the SRSs. Consequently, a balance between the network solutions and non-network solutions at multiple stages is achieved through iterations between the upper level and lower level, which simulates the information interaction process between planners and operators of ADN.

REFERENCES

[1] J. Zhao, Y. Wang, G. Song *et al.*, "Congestion management method of low-voltage active distribution networks based on distribution locational marginal price," *IEEE Access*, vol. 7, pp. 32240-32255, Mar. 2019.

[2] M. R. Haghifam, H. Falaghi, and O. P. Malik, "Risk-based distributed generation placement," *IET Generation, Transmission & Distribution*, vol. 2, no. 2, pp. 252-260, Mar. 2008.

[3] Y. Wang, N. Zhang, C. Kang *et al.*, "An efficient approach to power system uncertainty analysis with high-dimensional dependencies," *IEEE Transactions on Power Systems*, vol. 33, no. 3, pp. 2984-2994, May 2018.

[4] Q. Hou, E. Du, N. Zhang *et al.*, "Impact of high renewable penetration on the power system operation mode: a data-driven approach," *IEEE Transactions on Power Systems*, vol. 35, no. 1, pp. 731-741, Jan. 2020.

[5] G. Celli, S. Mocci, F. Pilo *et al.*, "Optimal integration of energy storage in distribution networks," in *Proceedings of 2009 IEEE Bucharest PowerTech*, Bucharest, Romania, Jul. 2009, pp. 1-7.

[6] J. Xiao, Z. Zhang, L. Bai *et al.*, "Determination of the optimal installation site and capacity of battery energy storage system in distribution network integrated with distributed generation," *IET Generation, Transmission & Distribution*, vol. 10, no. 3, pp. 601-607, Feb. 2016.

[7] S. Wang, Z. Dong, F. Luo *et al.*, "Stochastic collaborative planning of electric vehicle charging stations and power distribution system," *IEEE Transactions on Industrial Informatics*, vol. 14, no. 1, pp. 321-331, Jan. 2018.

[8] Y. Li, H. Zhang, X. Liang *et al.*, "Event-triggered-based distributed cooperative energy management for multienergy systems," *IEEE Transactions on Industrial Informatics*, vol. 15, no. 4, pp. 2008-2022, Apr. 2019.

[9] O. Sadeghian, M. Nazari-Heris, M. Abapour *et al.*, "Improving reliability of distribution networks using plug-in electric vehicles and demand response," *Journal of Modern Power Systems and Clean Energy*, vol. 7, no. 5, pp. 1189-1199, Sept. 2019.

[10] A. Keane, L. F. Ochoa, C. L. T. Borges *et al.*, "State-of-the-art techniques and challenges ahead for distributed generation planning and optimization," *IEEE Transactions on Power Systems*, vol. 28, no. 2, pp. 1493-1502, May 2013.

[11] M. A. Muhammad, H. Mokhlis, K. Naidu *et al.*, "Distribution network planning enhancement via network reconfiguration and DG integration using dataset approach and water cycle algorithm," *Journal of Modern Power Systems and Clean Energy*, vol. 8, no. 1, pp. 86-93, Jan. 2020.

[12] N. C. Koutsoukis, P. S. Georgilakis, and N. D. Hatziargyriou, "Multistage coordinated planning of active distribution networks," *IEEE Transactions on Power Systems*, vol. 33, no. 1, pp. 32-44, Jan. 2018.

[13] S. Haffner, L. F. A. Pereira, L. A. Pereira *et al.*, "Multistage model for distribution expansion planning with distributed generation – Part I: problem formulation," *IEEE Transactions on Power Delivery*, vol. 23, no. 2, pp. 915-923, Apr. 2008.

[14] M. Sedghi, A. Ahmadian, and M. Aliakbar-Golkar, "Optimal storage planning in active distribution network considering uncertainty of wind power distributed generation," *IEEE Transactions on Power Systems*, vol. 31, no. 1, pp. 304-316, Jan. 2016.

[15] X. Fang, F. Li, Y. Wei *et al.*, "Reactive power planning under high penetration of wind energy using Benders decomposition," *IET Generation, Transmission & Distribution*, vol. 9, no. 14, pp. 1835-1844, May 2015.

[16] X. Shen, M. Shahidehpour, S. Zhu *et al.*, "Multi-stage planning of active distribution networks considering the co-optimization of operation strategies," *IEEE Transactions on Smart Grid*, vol. 9, no. 2, pp. 1425-1433, Mar. 2018.

[17] Y. Gao, X. Hu, W. Yang *et al.*, "Multi-objective bilevel coordinated planning of distributed generation and distribution network frame based on multiscenario technique considering timing characteristics," *IEEE Transactions on Sustainable Energy*, vol. 8, no. 4, pp. 1415-1429, Oct. 2017.

[18] G. Muñoz-Delgado, J. Contreras, and J. M. Arroyo, "Multistage generation and network expansion planning in distribution systems considering uncertainty and reliability," *IEEE Transactions on Power Systems*, vol. 31, no. 5, pp. 3715-3728, Sept. 2016.

[19] Y. P. Agalgaonkar, B. C. Pal, and R. A. Jabr, "Stochastic distribution system operation considering voltage regulation risks in the presence of PV generation," *IEEE Transactions on Sustainable Energy*, vol. 6, no. 4, pp. 1315-1324, Oct. 2015.

[20] X. Fang, B. Hodge, F. Li *et al.*, "Adjustable and distributionally robust chance-constrained economic dispatch considering wind power uncertainty," *Journal of Modern Power Systems and Clean Energy*, vol. 7, no. 3, pp. 658-664, May 2019.

[21] M. Ahmadigorji, N. Amjady, and S. Dehghan, "A robust model for multiyear distribution network reinforcement planning based on information-gap decision theory," *IEEE Transactions on Power Systems*, vol. 33, no. 2, pp. 1339-1351, Mar. 2018.

[22] N. B. Arias, A. Tabares, J. F. Franco *et al.*, "Robust joint expansion planning of electrical distribution systems and EV charging stations," *IEEE Transactions on Sustainable Energy*, vol. 9, no. 2, pp. 884-894, Apr. 2018.

[23] Y. Li, D. Gao, W. Gao *et al.*, "Double-mode energy management for multi-energy system via distributed dynamic event-triggered Newton-Raphson algorithm," *IEEE Transactions on Smart Grid*, vol. 11, no. 6, pp. 5339-5356, Nov. 2020.

[24] Z. Zhuo, E. Du, N. Zhang *et al.*, "Incorporating massive scenarios in transmission expansion planning with high renewable energy penetration," *IEEE Transactions on Power Systems*, vol. 35, no. 2, pp. 1061-1074, Mar. 2020.

[25] H. Singh, S. Hao, and A. Papalexopoulos, "Transmission congestion management in competitive electricity markets," *IEEE Transactions on Power Systems*, vol. 13, no. 2, pp. 672-680, May 1998.

[26] L. Deng, Z. Li, H. Sun *et al.*, "Generalized locational marginal pricing in a heat-and-electricity-integrated market," *IEEE Transactions on Smart Grid*, vol. 10, no. 6, pp. 6414-6425, Nov. 2019.

[27] E. Celebi and J. D. Fuller, "Time-of-use pricing in electricity markets under different market structures," *IEEE Transactions on Power Systems*, vol. 27, no. 3, pp. 1170-1181, Aug. 2012.

[28] Z. Zhao, L. Wu, and G. Song, "Convergence of volatile power markets with price-based demand response," *IEEE Transactions on Power Systems*, vol. 29, no. 5, pp. 2107-2118, Sept. 2014.

[29] Z. Chen, Y. Sun, X. Ai *et al.*, "Integrated demand response characteristics of industrial park: a review," *Journal of Modern Power Systems and Clean Energy*, vol. 8, no. 1, pp. 15-26, Jan. 2020.

[30] Y. Hung and G. Michailidis, "Modeling and optimization of time-of-use electricity pricing systems," *IEEE Transactions on Smart Grid*, vol. 10, no. 4, pp. 4116-4127, Jul. 2019.

[31] R. Gholizadeh-Roshanagh and K. Zare, "Electric power distribution system expansion planning considering cost elasticity of demand," *IET Generation, Transmission & Distribution*, vol. 13, no. 22, pp. 5229-5236, Nov. 2019.

[32] M. Rey, S. M. de Oca, Á. Giusto *et al.*, "Distributed generation and demand response effects on the distribution network planning," in *Proceedings of 2018 IEEE PES Transmission & Distribution Conference and Exhibition-Latin America*, Lima, Peru, Sept. 2018, pp. 1-5.

[33] B. Zeng, J. Zhang, X. Yang *et al.*, "Integrated planning for transition to low-carbon distribution system with renewable energy generation and demand response," *IEEE Transactions on Power Systems*, vol. 29, no. 3, pp. 1153-1165, May 2014.

[34] M. Asensio, P. M. de Quevedo, G. Muñoz-Delgado *et al.*, "Joint distribution network and renewable energy expansion planning considering DR and energy storage–Part I: stochastic programming model," *IEEE Transactions on Smart Grid*, vol. 9, no. 2, pp. 655-666, Mar. 2018.

[35] M. Asensio, G. Muñoz-Delgado, and J. Contreras, "Bi-level approach to distribution network and renewable energy expansion planning considering DR," *IEEE Transactions on Power Systems*, vol. 32, no. 6, pp. 4298-4309, Nov. 2017.

[36] H. Yang, J. Zhang, J. Qiu *et al.*, "A practical pricing approach to smart grid demand response based on load classification," *IEEE Transactions on Smart Grid*, vol. 9, no. 1, pp. 179-190, Jan. 2018.

[37] PJM. (2019, Jul.). PJM manual 18: PJM capacity market. [Online]. Available: https://www.pjm.com/-/media/documents/manuals/m18.ashx

[38] J. A. Taylor and J. L. Mathieu, "Index policies for demand response," *IEEE Transactions on Power Systems*, vol. 29, no. 3, pp. 1287-1295, May 2014.

[39] D. Wang, K. Meng, X. Gao *et al*., "Optimal air-conditioning load control in distribution network with intermittent renewables," *Journal of Modern Power Systems and Clean Energy*, vol. 5, no. 1, pp. 55-65, Dec. 2016.

[40] F. Luo, Z. Dong, K. Meng *et al.*, "An operational planning framework for large-scale thermostatically controlled load dispatch," *IEEE Transactions on Industrial Informatics*, vol. 13, no. 1, pp. 217-227, Feb. 2017.

[41] Z. Bao, Q. Zhou, Z. Yang *et al.*, "A multi time-scale and multi energy-type coordinated microgrid scheduling solution – Part I: model and methodology," *IEEE Transactions on Power Systems*, vol. 30, no. 5, pp. 2257-2266, Sept. 2015.

[42] H. Zhang, Y. Li, D. Gao *et al.*, "Distributed optimal energy management for Energy Internet," *IEEE Transactions on Industrial Informatics*, vol. 13, no. 6, pp. 3081-3097, Dec. 2017.

[43] R. Romero, J. F. Franco, F. B. Leão *et al.*, "A new mathematical model for the restoration problem in balanced radial distribution systems," *IEEE Transactions on Power Systems*, vol. 31, no. 2, pp. 1259-1268, Mar. 2016.

[44] M. Lavorato, J. F. Franco, M. J. Rider *et al.*, "Imposing radiality constraints in distribution system optimization problems," *IEEE Transactions on Power Systems*, vol. 27, no. 1, pp. 172-180, Feb. 2012.

[45] W. F. Tinney, J. M. Bright, K. D. Demaree *et al.*, "Some deficiencies in optimal power flow," *IEEE Transactions on Power Systems*, vol. 3, no. 2, pp. 676-683, May 1988.

[46] P. Chen, X. Xiao, and X. Wang, "Interval optimal power flow applied to distribution networks under uncertainty of loads and renewable resources," *Journal of Modern Power Systems and Clean Energy*, vol. 7, no. 1, pp. 139-150, Jan. 2019.

[47] R. A. Jabr, R. Singh, and B. C. Pal, "Minimum loss network reconfiguration using mixed-integer convex programming," *IEEE Transactions on Power Systems*, vol. 27, no. 2, pp. 1106-1115, May 2012.

[48] H. Gao, R. Wang, Y. Liu *et al.*, "Data-driven distributionally robust joint planning of distributed energy resources in active distribution network," *IET Generation, Transmission & Distribution*, vol. 14, no. 9, pp. 1653-1662, May 2020.

[49] L. H. Macedo, J. F. Franco, M. J. Rider *et al.*, "Optimal operation of distribution networks considering energy storage devices," *IEEE Transactions on Smart Grid*, vol. 6, no. 6, pp. 2825-2836, Nov. 2015.

[50] M. Farivar and S. H. Low, "Branch flow model: relaxations and convexification – Part I," *IEEE Transactions on Power Systems*, vol. 28, no. 3, pp. 2554-2564, Aug. 2013.

[51] H. Xing, H. Cheng, L. Zhang *et al.*, "Second-order cone model for active distribution network expansion planning," in *Proceedings of 2015 IEEE PES General Meeting*, Denver, USA, Jul. 2015, pp. 1-5.

[52] Q. Li, R. Ayyanar, and V. Vittal, "Convex optimization for DES planning and operation in radial distribution systems with high penetration of photovoltaic resources," *IEEE Transactions on Sustainable Energy*, vol. 7, no. 3, pp. 985-995, Jul. 2016.

[53] X. Shen, M. Shahidehpour, Y. Han *et al.*, "Expansion planning of active distribution networks with centralized and distributed energy storage systems," *IEEE Transactions on Sustainable Energy*, vol. 8, no. 1, pp. 126-134, Jan. 2017.

Yixin Huang received the B.E. degree in electrical engineering from Zhejiang University, Hangzhou, China, in 2018, where she is currently pursuing the M.E. degree with the College of Electrical Engineering. Her research interests include power system planning and demand response.

Zhenzhi Lin received the Ph.D. degree in electrical engineering from the South China University of Technology, Guangzhou, China, in 2008. He was a Research Assistant with the Department of Electrical Engineering, Hong Kong Polytechnic University, Hong Kong, China, from 2007 to 2008, a Research Scholar with the Min Kao Department of Electrical Engineering and Computer Science, University of Tennessee, Knoxiville, USA, from 2010 to 2011, and a Research Associate with the School of Engineering and Computing Sciences, Durham University, Durham, UK, from 2013 to 2014. He is currently a Professor with the School of Electrical Engineering, Zhejiang University, Hangzhou, China. His research interests include power system wide area monitoring and control, controlled islanding, and power system restoration.

Xinyi Liu received the B.E. degree in electrical engineering from Shandong University, Jinan, China, in 2019. She is currently pursuing the M.E. degree with the College of Electrical Engineering, Zhejiang University, Hangzhou, China. Her research interests include electricity market and demand response.

Li Yang received the Ph.D. degree in electrical engineering from Zhejiang University, Hangzhou, China, in 2004. She was a Postdoctorate with the Department of Electrical Engineering, Turin Polytechnic University, Turin, Italy, from 2007 to 2008. She is currently an Associate Professor with the College of Electrical Engineering, Zhejiang University. Her research interests include power market, power system economics, and distribution network planning.

Yangqing Dan received the B.E. and Ph.D. degrees in electrical engineering from North China Electric Power University, Beijing, China, in 2012 and 2015, respectively. He is currently a Senior Engineer with the State Grid Zhejiang Economic Research Institute, Hangzhou, China. His research interests include power system planning and new energy integration system.

Yanwei Zhu received the B.E. and Ph.D. degrees in electrical engineering from North China Electric Power University, Beijing, China, in 2008 and 2012, respectively. She is currently a Senior Engineer with the State Grid Zhejiang Electric Power Co., Ltd., Ningbo Power Supply Company, Ningbo, China. Her research interests include power system operation and new energy scheduling.

Yi Ding received the B.E. degree from Shanghai Jiao Tong University, Shanghai, China, in 2000, and the Ph.D. degree from Nanyang Technological University, Singapore, Singapore, in 2007, both in electrical engineering. He is a Professor of reliability analysis and electricity market with the College of Electrical Engineering, Zhejiang University, Hangzhou, China. His current research interests include power system reliability, performance analysis incorporating renewable energy resources, smart grid, and reliability modelling and optimization of engineering systems.

Qin Wang received the B.S. degree from the Department of Electrical and Electronics Engineering, Huazhong University of Science & Technology, Wuhan, China, in 2006, the M.S. degree in electrical engineering from the South China University of Technology, Guangzhou, China, in 2009, and the Ph.D. degree from the Electrical and Computer Engineering Department, Iowa State University, Ames, USA, in 2013. He is currently a Senior Engineer/Scientist with Electric Power Research Institute, Palo Alto, USA. His previous industry experiences include positions with National Renewable Energy Laboratory, Midcontinent ISO and ISO New England. His research interests include power system reliability and online security analysis, smart distribution system, transactive energy, transmission planning, and electricity market.